Raman spectroscopy of silicon with nanostructured surface

Kadlečíková, Magdaléna; Vančo, Ľubomír; Breza, Juraj; Mikolášek, Miroslav; Hušeková, Kristína; Fröhlich, Karol; Procel, Paul; Zeman, Miro; Isabella, Olindo

DOI
10.1016/j.ijleo.2022.168869

Publication date
2022

Document Version
Final published version

Published in
Optik

Citation (APA)
Kadlečíková, M., Vančo, Ľ., Breza, J., Mikolášek, M., Hušeková, K., Fröhlich, K., Procel, P., Zeman, M., & Isabella, O. (2022). Raman spectroscopy of silicon with nanostructured surface. *Optik*, *257*, Article 168869. https://doi.org/10.1016/j.ijleo.2022.168869

Optik - International Journal for Light and Electron Optics 257 (2022) 168869

Contents lists available at ScienceDirect

Optik

journal homepage: www.elsevier.com/locate/ijleo

Raman spectroscopy of silicon with nanostructured surface

Magdaléna Kadlečíková [a], Ľubomír Vančo [b], Juraj Breza [a,*], Miroslav Mikolášek [a], Kristína Hušeková [c,d], Karol Fröhlich [c,d], Paul Procel [e], Miro Zeman [e], Olindo Isabella [e]

[a] Slovak University of Technology, Faculty of Electrical Engineering and Information Technology, Ilkovičova 3, 812 19 Bratislava, Slovakia
[b] Slovak University of Technology, Faculty of Materials Science and Technology, Vazovova 5, 812 43 Bratislava, Slovakia
[c] Centre for Advanced Materials Application, Slovak Academy of Sciences, Dúbravská cesta 5807/9, 845 11 Bratislava, Slovakia
[d] Institute of Electrical Engineering, Slovak Academy of Sciences, Dúbravská cesta 9, 841 04 Bratislava, Slovakia
[e] Photovoltaic Materials and Devices Group, Delft University of Technology, Mekelweg 4, 2628 CD Delft, the Netherlands

ARTICLE INFO

Keywords:
Black silicon
Nanolayer RuO_2-IrO_2
SERS

ABSTRACT

We compared the morphology and Raman response of nanoscale shaped surfaces of Si substrates versus monocrystalline Si. Samples were structured by reactive ion etching, and four of them were covered by a RuO_2-IrO_2 layer. Raman bands, centred at approx. 520 cm^{-1}, belonging to samples processed by etching the Si surface have intensities higher by approximately one order of magnitude than those of reference non-etched samples. For nanostructured samples, the rise in the Raman signal was 12–14 × , which is in agreement with the model of the electric field at the tips of Si due to their geometry. This phenomenon is related to the high absorption of excitation radiation. Nanostructured surfaces of samples containing a layer of RuO_2-IrO_2 give rise to the phenomenon of surface enhancement of the Raman response most likely due to the charge transfer at the interface between silicon and conductive oxides. The nanostructured surface of Si without a metal layer behaves as a SERS substrate and detects the analytes at a low concentration.

1. Introduction

Black silicon is silicon with a modified nanostructure of the surface. This nanostructured layer efficiently minimises light reflection in a wide range of wavelengths. Therefore, the surface appears black [1]. Recent experiments [2–4] have pointed to black silicon as a potential substrate for surface enhanced Raman spectroscopy (SERS) and tip-enhanced Raman spectroscopy (TERS). This is due to the possibility of its production with a large surface area and also due to the plentiful possibilities of its structuring. The simplest and most cost-effective SERS technique is the use of metal nanoparticles but the problem is poor controllability, stability and reproducibility of the substrate properties, leading to inconsistencies in the resulting SERS signals. Therefore, the study and research of nanostructured non-metallic SERS substrates is interesting not only for extending the applications of SERS but also for better understanding the fundamental physical mechanisms of the amplification mechanism [5–9].

Guilin Wang et al. [5] built SERS structures on a nanoporous silicon surface and a flexible polydimethylsiloxane film with silver particles. They studied the depth and pore size of porous silicon and achieved a five-fold amplification of the Raman signal on this non-metallic surface. Ramirez-Gutierrez et al. [6] present determination of porosity and roughness of porous silicon thin films. The

* Corresponding author.
E-mail address: juraj.breza@stuba.sk (J. Breza).

https://doi.org/10.1016/j.ijleo.2022.168869
Received 14 January 2022; Received in revised form 25 February 2022; Accepted 6 March 2022
Available online 11 March 2022

authors of extensive work [7] studied the effect of the pore depth of nanoporous silicon on the amplification of the Raman analyte signal. They observed that the Raman signal intensity of the analyte molecules increased continuously with increasing depth of silicon nanopores and increased by about a factor of two in the range of 40–220 nm. By further increasing the pore depth to 900 nm, the intensity of the Raman response decreased. The authors concluded that as the pore depth increased, the electromagnetic field became more localised. However, the intensity of the Raman signal decreased, which can be explained by increased light trapping. In this case, part of the Raman scattering light cannot escape from the nanopores, so it no longer carries the analyte information.

The authors of the richly cited work [8] investigated the influence of the surface morphology of the black silicon substrate on the detection of individual algal cells using SERS. By modifying the O_2 and SF_6 flows in the cryogenic plasma etching process, they created different surface morphologies of the silicon substrate. The black silicon was covered with a 400 nm layer of gold so that the tips were bridged. The intensity of the Raman response was found to increase as the density of the spikes increased. For a substrate with a density of 30 points/μm^2, the detection limit of the R6G solution was reached at 10 fM, individual algae (Chlorella vulgaris) cells were detected and the Raman signals of carotenoids and lipids were significantly increased. Mitsai et al. [9] designed a black Si substrate SERS with a size of 10×10 cm^2 fabricated by plasma etching technology. The substrate contained randomly spaced spikes. This was tested without a metal coating and by comparing the catalytic conversion of para-aminothiophenol (PATP) to 4,4′-dimercaptoazobenzene (DMAB). They achieved SERS detection at a concentration of 10^{-6} M.

To date, different types of silicon nanostructures have been investigated for SERS applications. However, several authors state that the role of the morphology of the nanostructured silicon surface in the Raman signal amplification mechanism is still unclear.

In this experimental work we use Raman spectroscopy to study nanostructured silicon in comparison with flat monocrystalline silicon. Both flat silicon and nanostructured silicon substrates are composed of the same material and the only difference between them is the morphology of the silicon surface. The main research task was to verify the surface amplification of the Raman signal of nanostructured silicon and to find if the nanostructured surface of Si without a metal layer behaves as a SERS substrate and detects the analyte at low concentration. Raman spectroscopy is an ideal technique for this application because it is simple, fast and mainly contactless. In addition, we report the morphology of the nanostructured surface of silicon with differential density and average of nanocones and covered with a layer of IrO_2-RuO_2, as well as an image of the analyte captured at the tips of the nanostructure.

2. Experiment

2.1. Preparation of samples

The eight studied samples are listed in Table 1. Two samples, RA and RB, are wafers of (100)-oriented single-crystalline n-type silicon, where sample RB was rinsed in HF so as to remove native oxide.

Samples D and Z are reference samples of black silicon. They were structured by reactive ion etching (RIE). In the case of sample D, also defect removal etching (DRE) was applied after RIE. This is a special mode of etching that partly blunts the tips and reduces the amount of electrically active defects at the interfaces of these structures. Samples DA, DB, ZA and ZB are samples of black silicon with a capping layer of RuO_2-IrO_2. The nanolayer of conductive RuO_2-IrO_2 oxide was deposited by metal-organic chemical vapour deposition (MOCVD) and atomic layer deposition (ALD).

A brief description of the technology follows. The double-side polished n-type (100)-oriented single crystal slices with a thickness of 285 ± 25 μm with native SiO_2 were used as substrates. The silicon substrates were immersed in diluted HF (2.5%) to remove the native oxide. Texturing of the surfaces, thus forming nanocones was carried out by RIE using a gaseous mixture of SF_6 and O_2. After RIE, standard cleaning, rinsing in deionized H_2O and drying of the substrates was carried out. This was followed by short DRE in a solution of tetramethylammonium hydroxide 1%-diluted in H_2O at room temperature for 160 s. Such etching was followed by cleaning, deionized H_2O rinsing, and drying. A SiO_2 layer was formed on the Si substrate in the ALD equipment by exposure to ozone at 300 °C. SiO_2 film with a thickness of ≈ 2.0 nm was grown using 200 cycles with 3 s duration. The growth of RuO_2-IrO_2 layers, approximately 5 nm thick, was performed by liquid injection of metal-organic chemical vapour deposition in a horizontal low pressure hot-wall reactor. Ru (thd) 2 (cod), bis (2,2,6,6-tetramethyl-3,5-heptanedione), acetylacetonato (1,5-cyclooctadiene) ruthenium, Ir (cod) (acac) and (1.5 -cyclooctadiene) iridium dissolved in isooctane with 0.03 M concentration were used as precursors in the deposition of the RuO_2-IrO_2 layer. The growth of RuO_2-IrO_2 films was conducted at a temperature of 300 °C at a pressure of 133 Pa. The method of producing black silicon used in this work was originally intended for the development of solar cells [10–14].

2.2. Characterisation methods

Morphology of the surfaces of nanostructured silicon substrates was observed by a scanning electron microscope JEOL JSM 7500F

Table 1
The studied samples of silicon.

Sample	RA	RB	D	Z	DA	DB	ZA	ZB
	Bare Si		Structured Si samples					
Etching in HF	NO	YES	NO	NO	NO	YES	NO	YES
MO CVD and ALD								
Deposition of 1.5 nm SiO_2 (ALD)	Samples without any deposition		NO	NO	YES	YES	YES	YES
Preparation of 5 nm RuO_2-IrO_2			NO	NO	YES	YES	YES	YES

equipped with a field emission electron source using a 15 kV accelerating voltage and a beam current of 20 μA. Images were taken in combined secondary and backscattered electron modes with sample-to-detector distance of approx. 7 mm. SEM characterised the shape and size of nanocones, their number and distribution. The number of nanocones was determined by image processing with the freely available code ImageJ. The histograms are constructed so that the grey-value of the pixels in each SEM image lies between 0 and

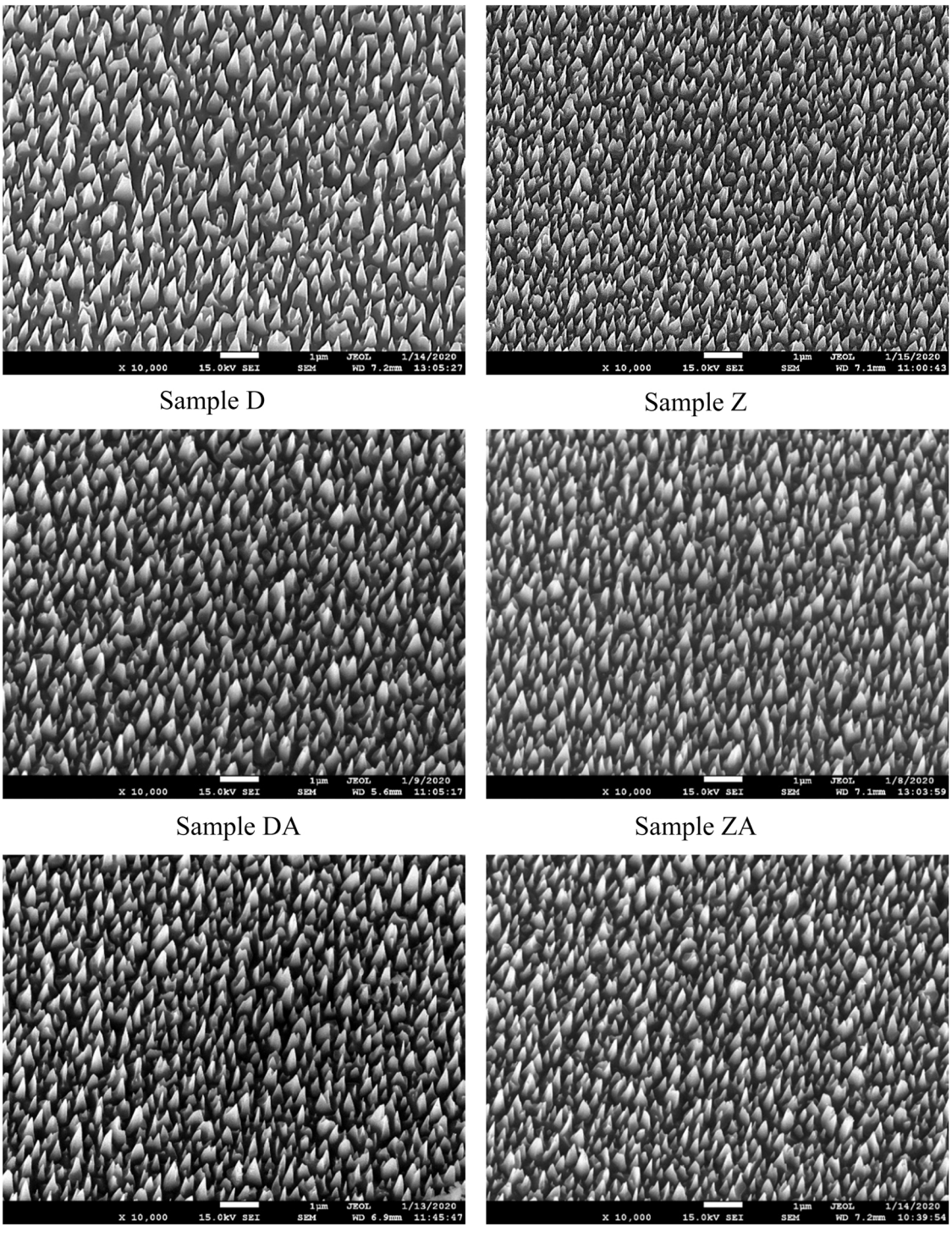

Fig. 1. Etched structures of Si surface viewed at an angle of 15°, magnification 10,000×.

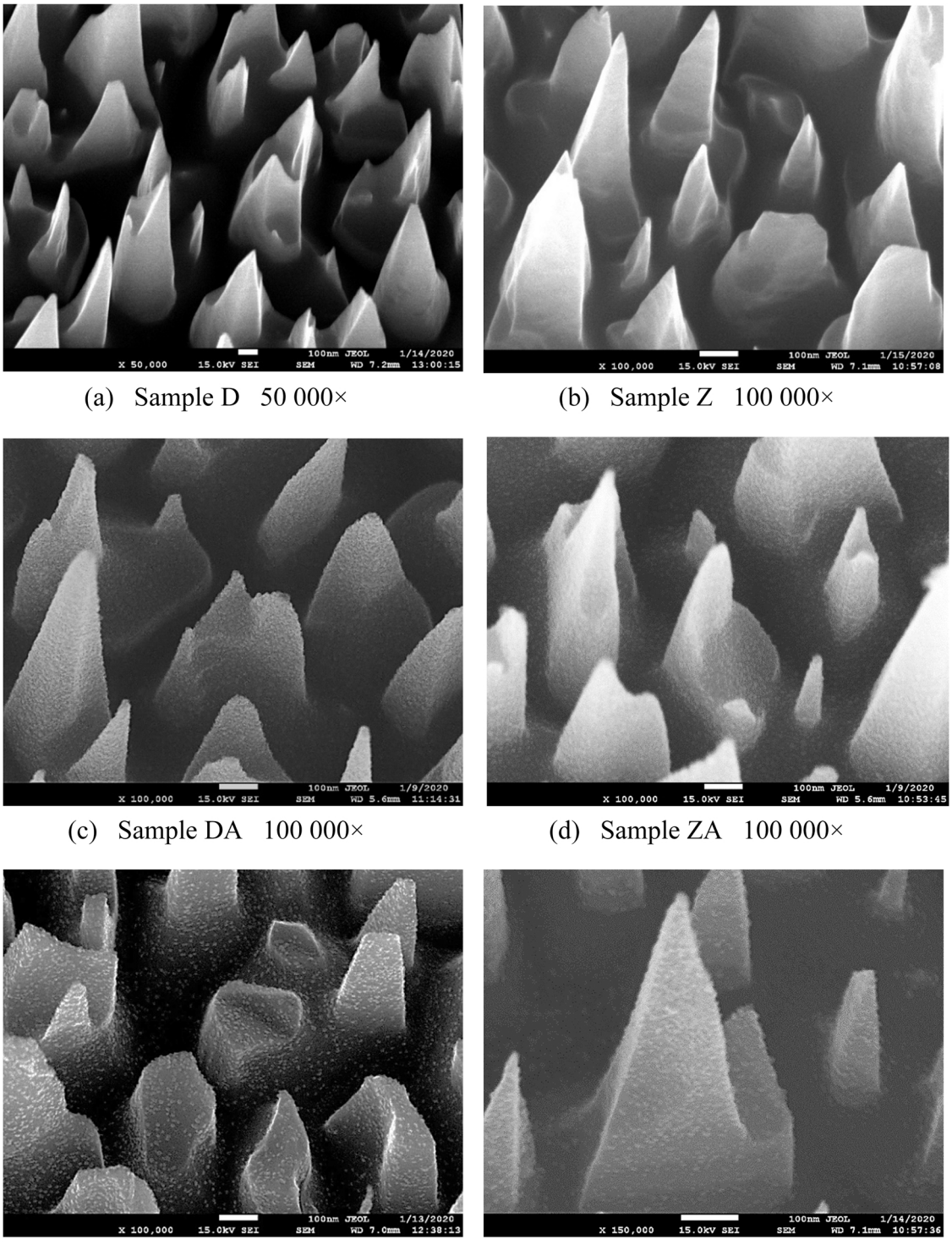

(a) Sample D 50 000× (b) Sample Z 100 000×

(c) Sample DA 100 000× (d) Sample ZA 100 000×

(e) Sample DB 100 000× (f) Sample ZB 150 000×

Fig. 2. SEM micrographs of the etch-formed structures of black Si taken at an aspect angle of 15°, magnifications 50,000× to 150,000×. (a, b) Detail views of samples D and Z. The structure does not contain the RuO_2-IrO_2 layer. (c, d, e, f) Samples DA, ZA, DB and ZB, the surface of black Si with a nanostructured layer of conductive RuO_2-IrO_2 oxides.

255 and the threshold is set to 50. The grey-value of 50 is typical for an already visible nucleus of the nanocone. The measurements of reflectivity (R) were carried out on a UV/VIS/NIR spectrometer Avantes AvaSpec ULS2048CL-EVO-RS with a deuterium-halogen light source Avantes AvaLight DHc in the specular reflection mode for spectral range from 200 to 1100 nm. The amount of absorbed light was then calculated as $1–R$. Raman spectra were acquired with a Horiba JobinYvon Labram 300 spectrometer with a He-Ne laser (632.8 nm), grating monochromator (1800 grooves/mm), spectral resolution better than 1.3 cm^{-1} and measurement range from 100 to 4000 cm^{-1}. The spectrometer was calibrated on the dominant band of Si at 520.7 cm^{-1} and on the natural diamond band at 1332 cm^{-1}.

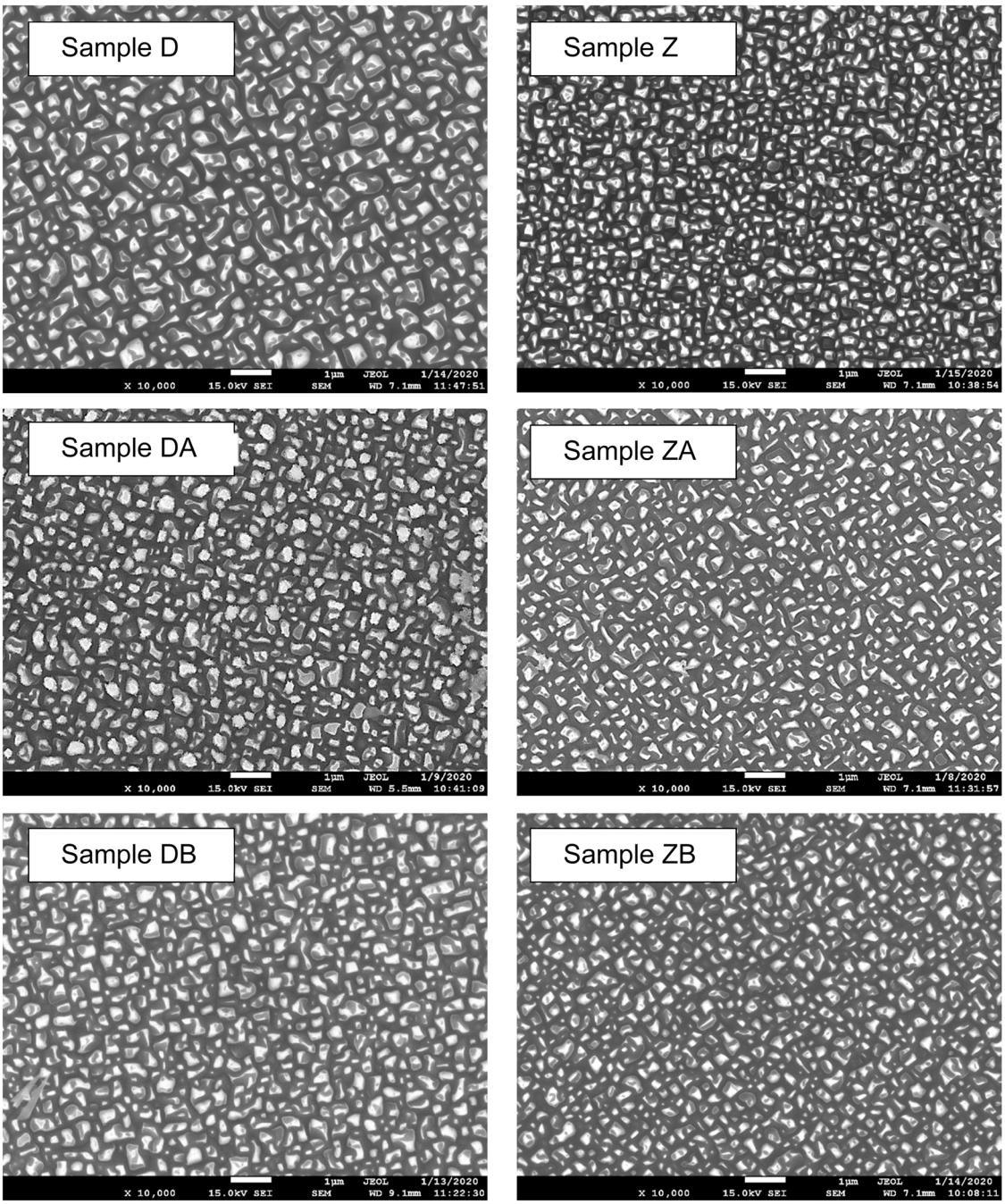

Fig. 3. Top-view SEM micrographs of nanocones.

3. Results and discussion

3.1. Scanning electron microscopy of nanostructured silicon

We compared the morphology of the shaped surfaces of individual Si substrates at 10,000× magnification, see Fig. 1. Details of the structures at magnifications 50,000–150,000× are shown in Fig. 2. SEM observations reveal that the etched Si structures are nanoscaled, both as for the height of the etched columns and their basic dimensions. Unlike in visualisations of the etched structures from other laboratories, for example nanowhiskers on p-type Si [15], the columnar structures we observed are several nanometres (up to 100 nm) apart and do not have a uniform pyramidal shape with a wide base. The etched segments vary in size and are also heterogeneous in shape. It is generally assumed that the formation of various nanopyramids, nanocups or nanopillars, *etc* during RIE is caused by local changes in the etching rate of Si. This variation in the etching rate may be due to the Si surface, for example an inhomogeneous oxide layer or incompletely removed native oxide. On the surfaces of the nanopyramids in Fig. 2, samples DA, DB, ZA and ZB show the structure of the conductive oxide layer. The conductive oxide layer has a granular or blister morphology with unequally sized grains. The grain size, as best seen in Fig. 2, sample DB, is approximately 2–10 nm.

3.2. Histograms of the densities of nanocones

SEM micrographs show that samples D, Z, DA, DB, ZA and ZB differ in the size of nanocones, in the tip densities and their amounts, see Figs. 3 and 4 and Table 2. Computer processing of the top view reveals the presence of islands. The nanocone distribution histograms are drawn in Fig. 4. The number of nanocones per unit area is markedly higher in samples Z, ZA and ZB than in samples D, DA and DB. Analysis of the Feret diameter of the nanocones did not reveal their preferred directional dimension.

3.3. Light absorption of studied silicon samples

As expected, in the range of visible light the samples (D, DA, DB, Z, ZA and ZB) are almost completely black. In the visible light, the light absorption of the studied black Si samples is close to 100%, as demonstrated by the shape of the absorption characteristics shown in Fig. 5. In the range from 380 nm to 780 nm, the absorption spectra of the samples of monocrystalline Si (samples RA and RB) measured in the specular reflectance setup show a slight deviation from the shape of the Si standard. The deviation is related to the cleaning of the surface of the samples, which was also observed by the Imamura et al. [17].

3.4. Raman spectra of nanostructured silicon

The strong Raman signal of Si at about 520 cm^{-1} is used to detect crystalline Si (c-Si), polycrystalline Si (poly-Si), amorphous Si (a-Si) as well as nanostructured silicon. This Raman band arises from the interaction of monochromatic light with the crystal lattice. It is described as the first order scattering on the phonon in the middle of the Brillouin zone (Γ) obeying the selection rule $|k| \approx 0$. The frequency of the Raman band corresponds to the frequency of phonons in Γ, which is 15.56 THz (520.7 cm^{-1}). The band is triple degenerate because three optical phonons take part in the scattering. Straight explanation of the mechanism of scattering is provided by Feynman diagrams. The Raman peaks of crystalline semiconductors are sharp because of the well-defined wave vectors of the phonons.

We focused on the Raman spectra in the spectral window from 510 cm^{-1} to 540 cm^{-1} containing the dominant Raman band of

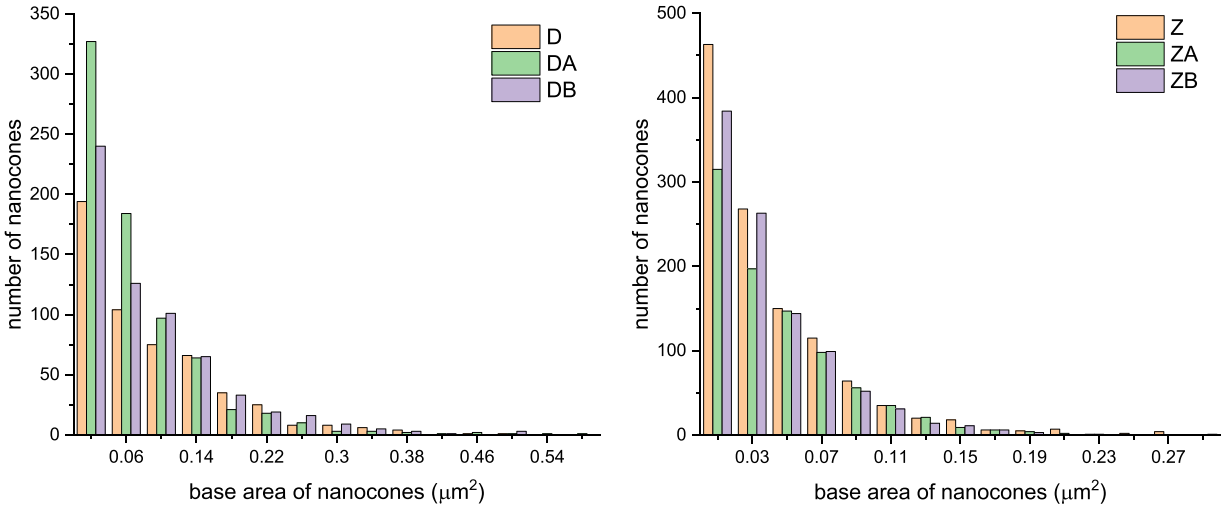

Fig. 4. Nanocone distribution histograms. The distribution is evaluated from SEM micrographs shown in Fig. 3 using software ImageJ.

Table 2
Density of nanocones and their average size.

Sample	Detected area coverage (%)	Density, number of nanocones per μm^2	Average base area of the nanocones (μm^2)
D	43.7	527	0.089
DA	47.7	718	0.069
DB	51.6	625	0.088
Z	45.5	1162	0.042
ZA	36.4	892	0.044
ZB	36.2	1008	0.039

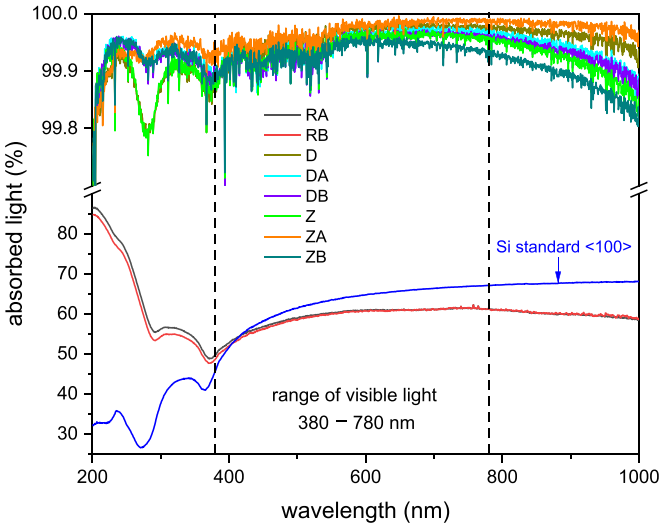

Fig. 5. Absorption spectra of samples D, DA, DB, Z, ZA, ZB of black silicon and of reference samples RA and RB of monocrystalline Si measured in the specular reflectance setup in the visible range at room temperature.

crystalline silicon centred at ≈ 520.7 cm^{-1}. The shape of this Raman band is characterised by its position, full width at half maximum height FWHM ≈ 3.5 cm^{-1} at room temperature [16] and intensity. The shape of the dominant Raman scattering band provides information about the deformation of the silicon crystal lattice, therefore its shape is also affected by the destruction of the material by etching. The Raman spectra of the structures of etched silicon (samples D and Z) and etched silicon with conductive oxide layer (samples DA, DB, ZA and ZB) are shown in Figs. 6 and 7 and compared with the Raman spectrum of unstructured silicon (samples RA and RB). The Raman spectra plotted in Fig. 6 were taken from the centre of each sample. The Raman spectra in Fig. 7 were taken from

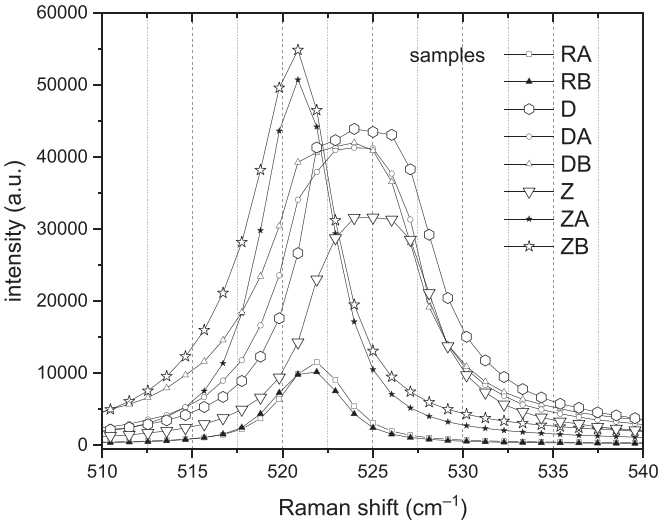

Fig. 6. Raman spectra of reference and nanostructured silicon taken in the centres of the samples.

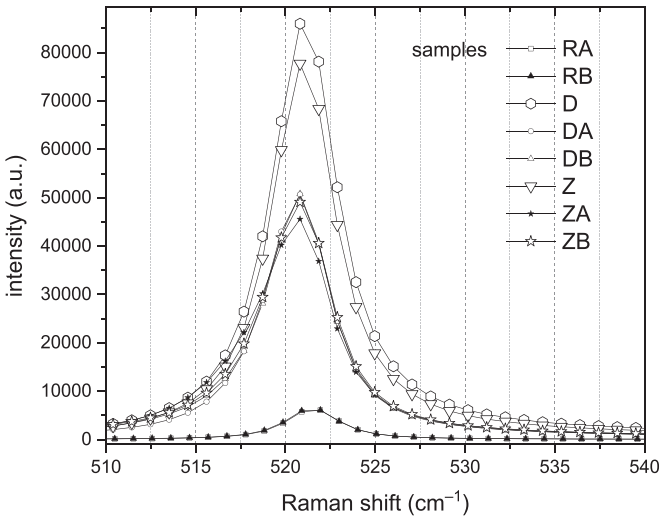

Fig. 7. Raman spectra of silicon samples with nanostructured surfaces at the spots arbitrarily selected outside the centre of the samples (6 measurements on each sample).

different locations on the samples. Table 3 shows the Raman intensity obtained by baseline correction and Lorentzian fitting of the peak at 520 cm^{-1} and the enhancement factor which characterises the ability of a given substrate to enhance the Raman signal. The reference samples for calculating the enhancement were RA or RB having the same intensity. In all samples with Si surface structured by etching (black silicon) the intensity of the dominant Raman band was higher compared to the intensity of the dominant Raman band of unstructured bulk monocrystalline Si.

Raman bands, centred at approx. 520 cm^{-1} belonging to samples processed by etching the structured Si surface (D, DA, DB, Z, ZA, ZB) have intensities higher by approximately one order of magnitude than the reference Si samples (RA and RB). For nanostructured samples D and Z, the rise in the Raman signal was 12–14 × , which is in agreement with the model the electric field at the tips of Si due to their geometry as established in [1]. This phenomenon is related to the high absorption of excitation radiation. The higher level of excitation radiation absorption ($\lambda = 632.8$ nm) of the black silicon samples D, DA, DB, Z, ZA and ZB is also evident from the comparison with the absorption spectra of the reference RA and RB samples Si in the visible region (Fig. 5). When comparing the absorption spectra of all black silicon samples, a minimal difference is observed between the absorption levels of the nanostructured (D and Z) and nanostructured (DA, DB, ZA and ZB) samples.

The rise in the Raman bands of the structured samples is attributed to two mechanisms. First, the enhancement in the Raman signal of nanostructured samples D and Z is due to increased emissions from silicon tips or countless reflections between the cavities of the nanocones. Nanostructured Si samples exhibit a high level of absorption and low level of reflectivity [17]. The intensity of the Raman response in the substrate is proportional to the intensity of light passing through it. However, we did not observe a relationship between the intensity of the Raman response and the density of nanocones.

Second, nanostructured surfaces (samples DA, DB, ZA and ZB) containing a layer of RuO_2-IrO_2 may give rise to the phenomenon of surface enhancement of the Raman response due to the induced charge transfer at the interface between silicon and conductive oxides. Ruthenium oxide and iridium oxide in nanostructured samples are only in the form of nanoparticles and absorb small portions of excitation light and scattered light but the RuO_2-IrO_2 nanolayers covering the nanostructured Si change the black silicon surface structure and hereby the physical properties of the interface. Therefore, they lead to an increase in the intensity of the Raman signal (samples DA, DB, ZA and ZB) compared to the intensity of the unstructured silicon surface of samples RA and RB. In Fig. 7, we observed a decrease in the intensity of the Raman signal (samples DA, DB, ZA and ZB) compared to the intensity of the black silicon of samples D and Z.

Table 3
Raman intensity of the band at ≈ 520 cm^{-1} and the enhancement factor of respective samples. RA and RB samples showing the same Raman characteristics were taken as a reference.

Sample	Raman intensity (a.u.)	Enhancement factor
RA	6030	1
RB	6030	1
D	85,260	14.1
DA	50,420	8.4
DB	50,300	8.3
Z	77,160	12.8
ZA	44,980	7.5
ZB	48,670	8.1

In the Raman spectra of structured Si samples, a shift of the dominant band to the side of both lower and higher wave numbers as well as an increase in FWHM are observed. The shift of the dominant band as well as the increase of FWHM can be caused by the stress created in the etched structure or also by combination of optical properties of the etched and non-etched places. Authors in [18–20] attribute the so-called Raman red shift (*ie* to the side of longer wavelengths) to the magnitude effect of silicon nanocrystals and the phenomenon of phonon vibrations closing in nanocrystals. FWHM increase is also attributed to this phenomenon in nanocrystals of various sizes.

It is interesting to compare the Raman bands of electrochemically etched porous Si structures published in [21] against the RIE etched structures analysed here. The electrochemically etched porous structured silicon surface deformed the dominant Raman band, reduced its intensity, and shifted the centre of the band to the lower wave numbers. On the other hand, RIE etched silicon surface increases the intensity of the dominant Raman band and shifts the centre of the band to the side of both lower and higher wave numbers.

3.5. SERS of nanostructured silicon without a metal layer

In our previous work [22,23] we have shown that the production of 3D SERS substrates or layered SERS substrates is technologically demanding.

Preparation of active substrates based on metals for SERS aims at creating a structure that contains, on the surface, metallic particles or a discontinuous layer with metallic fragments with nano dimensions below 100 nm. The highest amplification is achieved when the frequency of electron oscillation in the metal is close to the frequency of the primary laser radiation. It is generally accepted that the SERS enhancement factor of active substrates based on plasmonic metals depends on two decisive mechanisms: electromagnetic and chemical.

The mechanism of SERS on non-metallic surfaces has been less studied and elucidated than on metallic nanostructured surfaces [24–26]. In this work, we performed the SERS experiment on a sample of DA, to which we dripped a solution of rhodamine 6 G at a concentration of 10^{-4} M. The solvent was isopropyl alcohol. After free drying of the sample in air for 24 h, we conducted observations by SEM and Raman spectroscopy. Fig. 8 shows the SEM visualisation of rhodamine 6 G on nanocones of Si substrate, front view, with 15°aspect angle and 100,000× magnification. The captured Raman spectra in the spectral window from 1100 to 1700 cm^{-1} from seven sites of sample DA are shown in Fig. 9. The Raman spectra were not mathematically modified in any way. Bands at 1361 cm^{-1}, 1511 cm^{-1} and 1649 cm^{-1} are visible in the Raman spectrum. The recorded Raman bands clearly confirm the presence of rhodamine 6 G, despite the fact that there is a minimal amount of rhodamine 6 G at the tips and the layer is discontinuous. The amplification of the Raman intensity of R6G in SERS with a metal nanostructured layer can be explained on the basis of the phenomenon of localised plasmon resonance. For our SERS black Si substrates without a metal layer, the probable mechanism of amplification of the R6G Raman response is in combination of the effect of high levels of excitation radiation absorption and excitation of charge transfer at the Si and oxide interface in the RuO_2-IrO_2 nanolayer, as well as charge transfer at the RuO_2-IrO_2 interface and R6G molecules. This gives rise to the so-called tip effect, *ie* increased emission from the tips where R6G is captured. The sensitivity of SERS on a black Si-based substrate in our experiment is not sufficient to meet the requirement for practical detection applications. We believe that the SERS substrate based on black Si has the potential to identify trace amounts of substances or small concentrations of selected types of substances and also as a substrate for reproducible detection and characterisation of in situ processes in catalysis. RuO_2 has the function of a catalytic electrode in a photoelectrochemical cell. Effective improvement of the electrode surface stability is achieved by suitably added second metal oxide, such as IrO_2 in our case.

4. Conclusions

Raman bands with a centre at approx. 520 cm^{-1} recorded on black Si samples (D, DA, DB, Z, ZA, ZB) have intensities higher by one order of magnitude than those of monocrystalline Si samples (RA and RB).

The nanostructured surface of Si sample DA behaves as a SERS substrate without a metal layer and detects the analyte at a low concentration. The Raman spectra in the spectral window from 1100 to 1700 cm^{-1} of the nanostructured DA sample clearly confirmed the presence of rhodamine 6 G, despite the fact that the rhodamine 6 G layer is discontinuous and there is a minimum amount of this substance at the tips.

From the experimentally observed phenomena, we conclude that the mechanism of surface-enhanced Raman spectroscopy of the nanostructured Si surface is related to three facts:

- Nanostructured Si samples exhibit high absorption of radiation at $\lambda = 632.8$ nm and a low level of reflectance.
- Multiple reflections between nanocones and the so-called phonon trapping of radiation in silicon nanocrystals and consequent increased emission from the silicon tips.
- The existence of an interface and close contact between two oxides in the nanostructure RuO_2 covered with IrO_2 on Si. The structure containing the RuO_2-IrO_2 layer can bring about the phenomenon of surface enhancement due to charge transfer at the interface between silicon and the conductive oxides but also at the interface of RuO_2 and stable IrO_2.

Declaration of Competing Interest

The authors declare that they have no known competing financial interests or personal relationships that could have appeared to

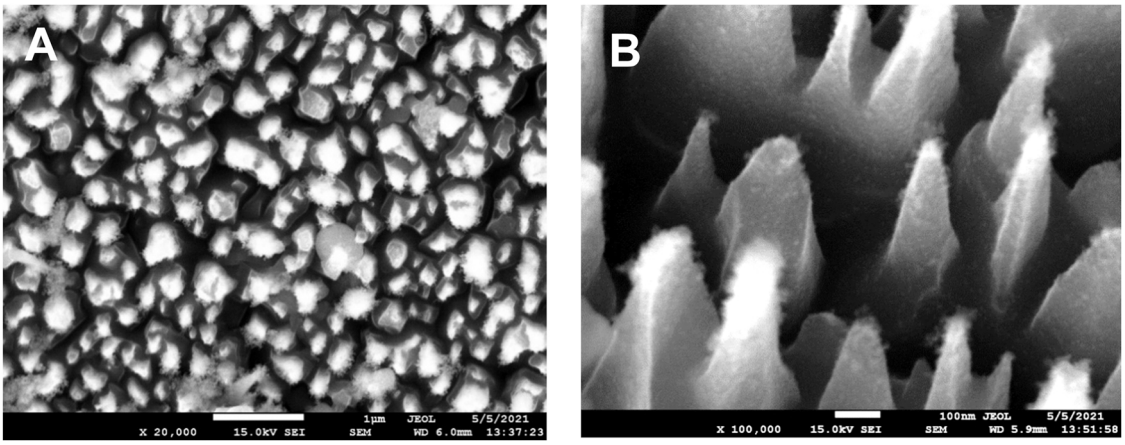

Fig. 8. (**A**) Top-view SEM image of Si structured by REI and decorated by rhodamine 6 G (isopropyl alcohol solution with concentration 10^{-4} M). (**B**) 15° tilted SEM image of Si structured by RIE with visible fragments of rhodamine 6 G at magnification 100,000×. Rhodamine does not create a continuous layer.

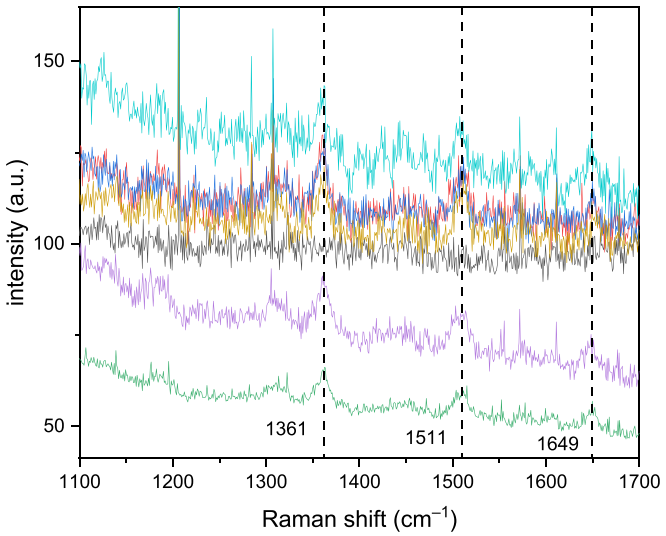

Fig. 9. Raman spectra of rhodamine 6 G taken at seven places of nanostructured black silicon, sample DA.

influence the work reported in this paper.

Acknowledgement

We are grateful to the Scientific Grant Agency of the Ministry of Education, Science, Research and Sport of the Slovak Republic for financial support of projects VEGA 1/0532/19 and VEGA 1/0529/20.

References

[1] Shijun Ma, Shuang Liu, Qinwei Xu, Junwen Xu, Rongguo Lu, Yong Liu, Zhiyong Zhong, A theoretical study on the optical properties of black silicon, AIP Adv. 8 (2018), 035010.
[2] G. Seniutinas, G. Gervinskas, R. Verma, B.D. Gupta, F. Lapierre, P.R. Stoddart, F. Clark, S.L. McArthur, S. Juodkazis, Versatile SERS sensing based on black silicon, Opt. Express 23 (2015) 6763–6772.
[3] Zhida Xu, Jing Jiang, Manas Ranjan Gartia, Gang Logan Liu, Monolithic integrations of slanted silicon nanostructures on 3D microstructures and their application to surface-enhanced Raman spectroscopy, J. Phys. Chem. C 116 (2012) 24161–24170.
[4] T.L. Vasconcelos, B.S. Archanjo, B.S. Oliveira, W.F. Silva, R.S. Alencar, C. Rabelo, C.A. Achete, A. Jorio, Optical nanoantennas for tip-enhanced Raman spectroscopy, IEEE J. Sel. Top. Quantum Electron. 27 (2021), 4600411-4600411.
[5] Guilin Wang, Ronghua Yi, Xueting Zhai, Renji Bian, Yongqian Gao, Dongyu Cai, Juqing Liu, Xiao Huang, Gang Lu, Hai Li, Wei Huang, A flexible SERS-active film for studying the effect of non-metallic nanostructures on Raman enhancement, Nanoscale 10 (2018) 16895–16901.

[6] C.F. Ramirez-Gutierrez, J.D. Castaño-Yepes, M.E. Rodriguez-Garcia, Porosity and roughness determination of porous silicon thin films by genetic algorithms, Optik 173 (2018) 271–278.
[7] Gang Lu, Guilin Wang, Hai Li, Effect of nanostructured silicon on surface enhanced Raman scattering, RSC Adv. 8 (2018) 6629–6633.
[8] Yu-Luen Deng, Yi-Je Juang, Black silicon SERS substrate: effect of surface morphology on SERS detection and application of single algal cell analysis, Biosens. Bioelectron. 53 (2014) 37–42.
[9] E. Mitsai, A. Kuchmizhak, E. Pustovalov, A. Sergeev, A. Mironenko, S. Bratskaya, D.P. Linklater, A. Balčytis, E. Ivanova, S. Juodkazis, Chemically non-perturbing SERS detection of a catalytic reaction with black silicon, Nanoscale 10 (2018) 9780–9787.
[10] B.W.H. van de Loo, A. Ingenito, M.A. Verheijen, O. Isabella, M. Zeman, W.M.M. Kessels, Surface passivation of n-type doped black silicon by atomic-layer-deposited SiO_2/Al_2O_3 stacks, Appl. Phys. Lett. 110 (2017), 263106.
[11] A. Ingenito, O. Isabella, M. Zeman: 19.8% conversion efficiency in modulated surface textured IBC c-Si solar cells, Proceedings of the Light, Energy and the Environment Conf. (2014) 1–3.
[12] E. Özkol, P. Procel, Y. Zhao, L. Mazzarella, R. Medlin, P. Šutta, O. Isabella, M. Zeman, Effective passivation of black silicon surfaces via plasma-enhanced chamical vapor deposition grown conformal hydrogenated amorphous silicon layer, Phys. Status Solidi RRL 14 (2020), 1900087.
[13] K. Fröhlich, V. Cambel, D. Machajdík, P.K. Baumann, J. Lindner, M. Schumacher, H. Juergensen, Low-temperature growth of RuO_2 films for conductive electrode applications, Mat. Sci. Semicond. Process. 5 (2003), 173–137.
[14] I. Brytavskyi, K. Hušeková, V. Myndrul, M. Pavlenko, E. Coy, K. Zaleski, D. Gregušová, L. Yate, V. Smyntyna, I. Iatsunskyi, Effect of porous silicon substrate on structural, mechanical and optical properties of MOCVD and ALD ruthenium oxide nanolayers, Appl. Surf. Sci. 471 (2019) 686–693.
[15] Zheng Fan, Danfeng Cui, Zengxing Zhang, Zhou Zhao, Hongmei Chen, Yanyun Fan, Penglu Li, Zhidong Zhang, Chenyang Xue, Shubin Yan, Recent progress of black silicon: from fabrications to applications, Nanomaterials 11 (2021) 41.
[16] H. Richter, Z.P. Wang, L. Ley, The one phonon Raman spectrum in microcrystalline silicon, Solid State Commun. 39 (1981) 625–629.
[17] K. Imamura, D. Irishika, H. Kobayashi, Mechanism of ultra-low reflectance for nanocrystalline Si/crystalline Si structure formed by surface structure chemical transfer method, J. Appl. Phys. 121 (2017), 013107.
[18] V. Paillard, P. Puech, M.A. Laguna, R. Carles, B. Kohn, F. Huisken, Improved one-phonon confinement model for an accurate size determination of silicon nanocrystals, J. Appl. Phys. 86 (1999) 1921–1924.
[19] G. Faraci, S. Gibilisco, A.R. Pennisi, C. Faraci, Quantum size effects in Raman spectra of Si nanocrystals, J. Appl. Phys. 109, 074311.
[20] G. Faraci, S. Gibilisco, P. Russo, A.R. Pennisi, S.L. Rosa, Modified Raman confinement model for Si nanocrystals, Phys. Rev. B 73 (2006), 033307.
[21] M. Kadlečíková, J. Breza, Ľ. Vančo, M. Mikolášek, M. Hubeňák, J. Racko, J. Greguš, Raman spectroscopy of porous silicon substrates, Optik 174 (2018) 347–353.
[22] Ľ. Vančo, M. Kadlečíková, J. Breza, M. Vojs, P. Michniak, M. Marton, Interference enhancement in SERS spectra of rhodamine 6G: relation to reflectance, Vib. Spectrosc. 90 (2017) 31–37.
[23] M. Kadlečíková, Ľ. Vančo, J. Breza, M. Vojs, P. Michniak, Two types of active substrates with silver nanostructured surfaces for surface enhanced Raman spectroscopy (SERS), ElectroScope 3 (2016) 4. ISSN 1802-4564.
[24] Shan Cong, Xiahong Liu, Yuxiao Jiang, Wei Zhang, Zhigang Zhao, Surface enhanced Raman scattering revealed by interfacial charge-transfer transitions, Innovation 1 (2020), 100051.
[25] Li-Hua Liu, Shao-Hui Cui, Ting-Zhao Fu, Yan Yuan, Chao-Bo Li, Effect of concentration on the position of fluorescence peak based on black-silicon SERS substrate, Appl. Surf. Sci. 464 (2019) 337–343.
[26] Jian Lv, Ting Zhang, Peng Zhang, Yingchun Zhao, Shibin Li, Review application of nanostructured black silicon, Nanoscale Res. Lett. 13 (2018) 110.